(p=0.07). In addition, stent eccentricity was positively correlated with area of calcium (p< 0.01). Among the 4 predefined groups, stent expansion defined by MSD was significantly different (p=0.02) (Figure). Stent expansion defined by MSA showed a similar trend (p=0.16).

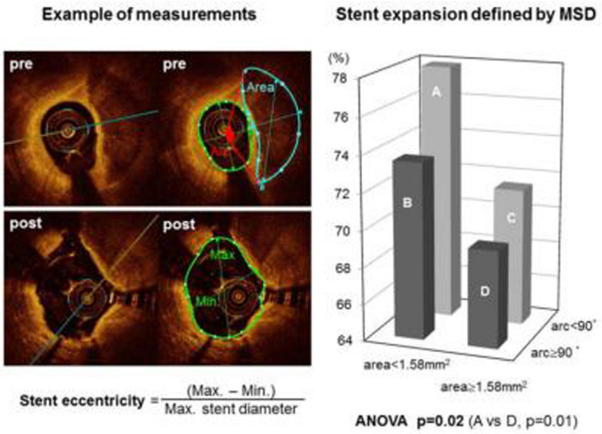

Conclusions: The amount of coronary calcium as assessed by OCT may predict stent expansion. Area of calcium appers to be a contributing factor for eccentric stent expansion.

TCT-386

Cut-plane Analysis: A new method of three-dimensional OCT rendering for side-branch ostial assessment from a main vessel pullback

Antonios Karanasos[1], Shengxian Tu[2], Nienke S. van Ditzhuijzen[3], Jurgen Ligthart[4], Nicolas M. Van Mieghem[5], Robert J. Van Geuns[5], Peter De Jaegere[6], Felix Zijlstra[7], Johan H. Reiber[8], Evelyn Regar[9]
[1]Thoraxcenter, Erasmus MC, Rotterdam, Zuid Holland, [2]Division of Image Processing, Department of Radiology, Leiden University Medical Center, Leiden, Leiden, [3]Erasmus University Medical Centre, Rotterdam, Zuid-Holland, [4]Erasmus MC Rotterdam, Rotterdam, Netherlands, [5]Erasmus MC, Rotterdam, Netherlands, [6]Thoraxcenter, Erasmus Medical Center, Rotterdam, Rotterdam, Netherlands, [7]Erasmus University Medical Center, Rotterdam, Netherlands, [8]Leiden University Medical Center, Leiden, Netherlands, [9]Thoraxcenter, Rotterdam, Netherlands

Background: In the assessment of coronary bifurcations, evaluation of side branch (SB) ostia by an optical coherence tomography (OCT) pullback performed in the main branch(MB) could speed up lesion evaluation. This assessment can be performed through dedicated software that renders the imaged segment in 3-D and reconstructs the cross-sections perpendicular to the SB centerline (cut-plane analysis). We aimed to validate these cut-plane analysis measurements of the SB ostium against reference measurements from a SB OCT pullback.
Methods: Thirty-one sets of frequency-domain OCT pullbacks from 28 patients, from both the MB and the SB of a coronary artery bifurcation were analyzed. Measurements of the SB ostium from the MB pullback were performed by 1)conventional analysis and 2)cut plane analysis, and the measurement error for each analysis versus reference measurements of the SB ostium from the SB pullback was estimated. We further analyzed an additional series of 12 consecutive sets of MB and SB pullbacks, in which SB ostium is not completely visualized in the MB pullback, in order to show the feasibility of imaging in this population.
Results: Correlations of SB ostium measurements acquired from the MB pullback in comparison to reference measurements acquired from the SB pullback, were higher with cut-plane analysis than with conventional analysis, albeit not reaching significance (area: $r_{cutplane}$=0.93 vs. $r_{conventional}$=0.87, p=0.26). Cut-plane analysis was associated with lower absolute error for SB ostium measurements than conventional analysis (area: 0.56±0.45mm^2 vs. 1.50±1.31mm^2, p< 0.001). Intra- and inter-observer agreement for cut plane analysis was high. In the additional set of images without complete SB ostium visualization, the correlation coefficient of SB area by cut-plane analysis and reference measurements was 0.88.
Conclusions: Area measurements of SB ostium performed by cut-plane analysis of an OCT pullback performed in the MB have high correlation with reference measurements performed from a SB OCT pullback and lower error compared to conventional analysis. This approach could potentially reduce procedural complexity in assessment of bifurcations.

TCT-387

Diagnostic Accuracy Of Optical Coherence Tomography Compared To Fractional Flow Reserve For The Severity Assessment Of Coronary Lesions: A Bivariate Meta-analysis

Georgios Siontis[1], Lorenz Raber[2], Konstantinos Siontis[3], Peter Jüni[4], Stephan Windecker[1]
[1]Bern University Hospital, Bern, Switzerland, [2]University Hospital Bern, Bern, Switzerland, [3]Mayo Clinic, ROCHESTER, MN, [4]University of Bern, Bern, Switzerland

Background: Optical coherence tomography (OCT) has emerged as a useful diagnostic tool for the evaluation of native and restenotic coronary artery lesions. However, the diagnostic accuracy of OCT in identifying hemodynamically significant coronary stenoses has not been well described.
Methods: We performed an electronic search of the PubMed, Cochrane Libraries, and EMBASE databases to identify eligible studies reporting lesion-level information on different OCT metrics (minimum lumen area (MLA), minimal lumen diameter (MLD), and % area stenosis (AS)). Using fractional flow reserve (FFR)=0.80 as reference for the definition of hemodynamically significant stenosis, we calculated sensitivities, specificities and utilized random-effects bivariate meta-analysis model to calculate summary diagnostic metrics and fit hierarchical summary receiver-operating characteristic (HSROC) curves according to different cutoffs of MLA (2.0, 3.0, 4.0 mm2), MLD (1.5, 1.75, 2.0 mm), and %AS (50 and 70%).
Results: Nine studies with lesion-level data for 458 coronary lesions in 337 patients were included. The medians (interquartile ranges) of MLA, MLD, and %AS were 2.25 mm2 (1.45-3.58), 1.50 mm (1.16-1.92) and 71% (61-76), respectively. For a cutoff of 2.0 mm2, MLA yielded the best combination of summary sensitivity 73% and specificity 85%, while the area under the HSROC curve was 0.85. MLD had high sensitivity for all examined thresholds (85%, 86% and 98% for 1.5, 1.75, and 2.0mm, respectively) and moderate to low specificity (65%, 43%, and 19%, respectively). The areas under the HSROC curves for the same thresholds were 0.85, 0.82 and 0.89, respectively. OCT-derived %AS of >50% resulted in excellent identification of hemodynamically severe coronary artery lesions (area under the HSROC curve of 0.98), however the specificity was very low (14%). A threshold of 70% for %AS resulted in area under the HSROC curve of 0.74 and improved specificity (70%).
Conclusions: In this bivariate meta-analysis, OCT metrics were highly sensitive across different cutoff values and yielded large areas under HSROC curves. Specificity, however, was low for detection of hemodynamically significant coronary lesions on most occasions.

TCT-388

Serial optical coherence tomography imaging of early atherosclerosis progression in diabetic versus non-diabetic swine

Nienke S. van Ditzhuijzen[1], Mieke van den Heuvel[1], Oana Sorop[1], Stefan Roest[1], Jurgen Ligthart[1], Felix Zijlstra[1], Dirk-Jan Duncker[1], Heleen v Beusekom[1], Evelyn Regar[1]
[1]Erasmus University Medical Center, Rotterdam, Netherlands

Background: Diabetic patients are at increased risk for adverse coronary events. Accelerated atherosclerosis progression may play an important pathogenic role. We compared the incidence of atherosclerotic coronary changes and their progression using an atherosclerotic swine model with diabetes mellitus (DM) versus without diabetes mellitus (NDM). Serial OCT imaging was used to monitor coronary changes in vivo over time.
Methods: In this longitudinal study, 12 male swine [n=7 DM, n=5 NDM] fed a high-cholesterol diet underwent serial coronary OCT at 9 and 12 months (M). A subgroup of 6 swine [n=3 DM, n=3 NDM] underwent additional OCT at 15M. The region of interest (ROI) was defined by the most distal until the most proximal segment of the coronary in which OCT was available at all time points. Within the ROI, lesions were classified according to plaque composition. Per lesion, mean no. quadrants and length of the lesion were determined, and a lesion index was calculated as [(mean no. quadrants*lesion length)/ROI].
Results: At 9M, DM swine showed predominantly early atherosclerosis with focally distributed eccentric intimal thickening (43%). In 14% a healthy vessel wall was observed, while in the NDM swine a healthy vessel wall was observed in the majority (60%). From 9 to 12M, atherosclerosis progressed faster in DM than NDM swine. Mean fibrous and lipid lesion index increased more in DM than NDM swine: fibrous 0.12±0.17 to 0.54±0.76 in DM and 0.02 (n=1 swine) to 0.17±0.08 in NDM, lipid 0.49±0.68 to 1.22±0.36 in DM and 0.42 to 0.54±0.03 in NDM swine. Likewise, late atherosclerosis progression from 9 to 15M was also sligthly faster in DM swine, mainly observed as an increase in mean lipid lesion index (0.02 to 1.35 (n=1 swine) in DM and 0 to 0.43±0.21 in NDM), rather than change in fibrous lesion index (0.17±0.21 to 0.15±0.05 in DM and 0.02 (n=1 swine) to 0.33±0.11 in NDM).
Conclusions: DM and NDM swine fed a high-cholesterol diet for 15M gradually develop coronary atherosclerosis similar to that seen in humans. In the DM swine, progression of early atherosclerosis was more accelerated than in NDM swine.